THE ASTRONOMICAL JOURNAL VOLUME 111, NUMBER 2 FEBRUARY 1996

THE GALAXY MOTION RELATIVE TO NEARBY GALAXIES AND THE LOCAL VELOCITY FIELD

I. D. KARACHENTSEV[1] AND D. A. MAKAROV

Special Astrophysical Observatory, Russian Academy of Sciences, N. Arkhyz, Zelenchukskaja, Stavropolsky Kraj, 357147, Russia
Electronic mail: ikar@sao.stavropol.su, dim@sao.stavropol.su

Received 1995 May 2; revised 1995 November 7

ABSTRACT

We consider a sample of 103 galaxies with radial velocities V_0<500 km s^{-1} and distances obtained by means of photometric distance indicators: Cepheids (n=17), brightest stars (n=69), and galaxy membership in the nearby bound groups (n=17). Ranking the galaxies with their distance R we determine a running apex for the Sun, the Galaxy, and the Local Group as a function of R. For the solar apex with respect to the LG galaxies we obtain the parameters: $\{l_\odot=93°\pm2°,\ b_\odot=-4°\pm2°,\ V_\odot=316\pm5$ km s$^{-1}\}$. That corresponds to a Galaxy center apex $\{l=107°,\ b=-18°,\ v=90$ km s$^{-1}\}$, pointing at ~14° from M31. When the considered volume depth increases from 1.0–1.5 Mpc up to 4–8 Mpc, the solar apex drifts to $\{l_\odot=91°,\ b_\odot=0°,\ V_\odot=334$ km s$^{-1}\}$, while the LG centroid apex shows a complicate wandering in a region $\{l=[40°, 100°],\ b=[0°, +60°]\}$ with velocity increasing from 0 up to 40 km s^{-1}. The running value for the local Hubble parameter, $H(R)$, reaches the maximum (90±5) km s^{-1} Mpc^{-1} at R~2 Mpc, and then decreases down to (70–65) km s^{-1} Mpc^{-1}. When both the Hubble component and the apex velocity are removed, the residual velocity field shows clear signs of anisotropy. Within the Local Supergalactic plane there is a prevalence of negative peculiar velocities towards the "+SGY" direction. This feature perhaps has the same origin as the "Local Velocity Anomaly" (LVA) known to exist over a scale of 10–30 Mpc. Besides the LVA, an excess of negative peculiar velocities is seen also along the SGZ axis and can be interpreted as if the expansion of the local pancake proceeds about 30% slower in the direction perpendicular to the symmetry plane than in the plane itself. Inside the Local Volume, galaxies possess a peculiar velocity dispersion of (72±2) km s^{-1} independent on the assumed volume depth. This value is almost the same for dwarf and giant galaxies: a behavior which has no simple explanations. The use of more precise solar apex parameters and the correction for the local anisotropy improves the use of radial velocities of nearby galaxies as distance indicators and allows to build a more accurate 3D map of the LV which reveals more "fine grain" structure details than Tully's catalog data.

I. INTRODUCTION

The Sun and our Galaxy take part in motions having different amplitudes and directions on the sky. With respect to its neighborhood stars the Sun has a peculiar velocity of 16 km s^{-1} in direction l=53°, b=25°. When combined to the galactic rotation ($V_{\rm rot}$=220±15 km s^{-1}, $\{l=90°,\ b=0°\}$ it leads to the apex parameters $\{l=87.°8,\ b=+1.°7\}$, V=232 km s^{-1} (de Vaucouleurs 1983; de Vaucouleurs *et al.* 1991). On the other hand, the Galaxy center possesses a peculiar velocity relative to the Local Group Centroid of about 100 km s^{-1} directed towards the nearest massive neighbour, M31 (Yahil *et al.* 1977). Next, the Local Group together with other nearby galaxy systems participates in a bulk motion toward the Local Supercluster center (Virgocentric flow) with a characteristic amplitude of ~250 km s^{-1} (Tonry & Davis 1981; Aaronson *et al.* 1982; Hoffman & Salpeter 1982). Finally, in the rest frame of the Cosmic Microwave Background (CMB) a viewing volume filled by galaxies reveals a large scale streaming towards the so-called "Great Attractor" with a velocity of ~600 km s^{-1} (Dressler *et al.* 1987; Lynden-Bell *et al.* 1988). The maximum scale of this cosmic "draught" is not yet established. Observational data on the bulk motions of galaxies on a scale of ~100 Mpc are at present still unreliable and even controversial (Mathewson *et al.* 1992; Lauer & Postman 1992). It has to be stressed, however, that also the motions of galaxies on a scale smaller than 10 Mpc are insufficiently known.

As Peebles (1988, 1989, 1994) emphasized, the knowledge of accurately measured distances and radial velocities of the nearby galaxies allows us to extrapolate their trajectories into a past, and therefore to make a choice between different scenarios of galaxy formation. Such a goal seems unfortunately to be still "*a nice dream*" since the distances of most nearby galaxies are either unknown or estimated with a low accuracy. This, for instance, is confirmed by the distance moduli obtained for IC 342, and Ho IX by different observers, which present a scatter of over than 2–3 mag. Difficulties in estimating distances lead to incompleteness and heterogeneity of their present data.

High accuracy distance moduli obtained from Cepheids

[1]Visiting astronomer at the Astronomical Observatory of Capodimonte, via Moiariello 16, I-80131 Napoli, Italy.

 0004-6256/96/111(2)/794/10/$6.00

are known only for a dozen of galaxies (Madore & Freedman 1991; Capaccioli & Piotto 1995). An application of the "luminosity–H I linewidth" relation (Tully & Fisher 1977) to the nearby objects does not yield reliable moduli, so far as a distance limited sample is preferably populated by dwarf irregular galaxies, whose scatter on the Tully–Fisher diagram (TF) is wider than for normal spirals. Other extragalactic distance indicators such as planetary nebulae, supernova bursts, or surface brightness fluctuations, require much observing time, and have not yet been applied to a large enough sample.

Therefore, in what follows, we shall study the local velocity field of galaxies, relying only on photometric distance moduli obtained mostly by means of the luminosity of the brightest blue and red supergiants.

2. THE OBSERVATIONAL SAMPLE

Kraan-Korteweg & Tammann (1979) compiled a list of nearby galaxies, with corrected radial velocities, $V_0 = V_h + 300 \sin l \cos b$, not exceeding 500 km s^{-1}. Over the whole sky, except the 6° zone around the Virgo cluster center, the above authors list 172 such objects. This sample has been increased to 215 by Karachentsev (1994) through the addition of new galaxies with recently measured radial velocities. In this supplement of data we found some cases of confusion and obvious errors in V_h. Finally, we added three new galaxies: Cas 1, Cas 2, and UGC 11583 (Huchtmeier 1994).

During the last four years a systematic CCD survey of northern galaxies in the sample has been undertaken at the 6 m telescope of Russian Academy of Sciences with the purpose to resolve them into stars and derive their photometric distance moduli. At present this project is 60% complete.

The available photometric moduli for galaxies in the sample have been summarized in (Karachentsev 1994), and (Karachentsev & Tikhonov 1994). In this work we also use new distance moduli for 21 dwarf galaxies, and also the mean distances for 17 galaxies which are members of bound groups according to the membership criterion recently introduced by Karachentsev (1994). The present work is therefore based on 103 galaxies, most of which are concentrated in the northern hemisphere. We believe the standard error of distance modulus for the sample is of 0.5 mag (or 25%).

The sample galaxies are listed in Table 1 in order of increasing distances. In column name: we give the galaxy identification; in columns l and b: the galactic coordinates and, in column V_h: the heliocentric radial velocity in km s^{-1}. With the exception of a few cases, the V_h are taken from the PGC catalogue (Paturel *et al.* 1992). Distance estimates (in Mpc) are indicated in column R. Galaxies with distances obtained via the group mean are marked by the letter "m." Preliminary distance estimates (Georgiev *et al.* 1996) are marked by the letter "p." Additional comments are presented in the table footnotes. The other columns in the table will be described in the next paragraph.

It must be emphasized that the present data base overlaps little with samples provided by other authors. For instance, de Vaucouleurs & Peters (1984) analyzed the solar motion relative to a sample of 600 galaxies having secondary distance estimates obtained from the luminosity index and the TF relation in the range of 2–50 Mpc. Their list has 15 galaxies in common with ours. For some of them, like M101 and Ho IV, the difference of moduli exceeds 1.5 mag. We do not discuss here the reason for such differences. Note, however, that the distance modulus of M101 derived by Cook *et al.* (1986) from Cepheids, (29.26 mag) agrees much better with our estimate (29.19 mag, KKK94) than with (VP94). Peebles (1988) studied the local velocity field using 47 galaxies with "cosmological" distances $cz < 900$ km s^{-1}. His list has only five galaxies in common with ours. A negligible amount of intersection between the data used by us and all other samples gives us a reason to reconsider the problem of solar motion and peculiar velocity field of the nearby galaxies.

3. RUNNING APEX OF THE SUN, THE GALAXY, AND THE LOCAL GROUP

For each galaxy with galactic coordinates l_i, b_i ranked in Table 1 according to its distance R_i we determine the directing cosines:

$$\begin{aligned} x_i &= \cos b_i \cos l_i, \\ y_i &= \cos b_i \sin l_i, \\ z_i &= \sin b_i. \end{aligned} \tag{1}$$

Components of solar velocity $V_{\odot x}$, $V_{\odot y}$, $V_{\odot z}$ to an apex with respect to the centroid of k nearest galaxies are calculated from the condition

$$\min\left\{ \sum_{i=1}^{k} (x_i V_{\odot x} + y_i V_{\odot y} + z_i V_{\odot z} + V_i - H R_i)^2 \right\}, \tag{2}$$

where V_i is the measured radial velocity of a galaxy and H is the local value of the Hubble parameter. By solving a linear regression on four variables: $V_{\odot x}$, $V_{\odot y}$, $V_{\odot z}$, and H, we can derive the modulus of solar velocity towards the apex, $V_\odot^2 = V_{\odot x}^2 + V_{\odot y}^2 + V_{\odot z}^2$, and the apex position on the sky in galactic coordinates: $l_\odot = \arctan(V_{\odot y}/V_{\odot x})$, $b_\odot = \arcsin(V_{\odot z}/V_\odot)$. The nearest galaxies, *id est* when $R_i < R_0$, do not take part in the cosmologic expansion, and we can assume $H = 0$. We also assume the radius of the "zero velocity surface" to be $R_0 = 1.5$ Mpc (Sandage 1986).

The derived solar apex parameters are given in the columns (solar apex) of Table 1, together with a running number "k" giving the number of galaxies considered. The drift of the solar apex with the sample depth is shown in Fig. 1 as a sequence of open circles joined each other. The large crossed circle indicates the direction of the Sun motion due to its galactic rotation and peculiar velocity as a star. Six other large circles mark the positions of the solar apex with respect to the members of the Local Group (LG) according to data by different authors. These apex parameters are listed in the top part of Table 2. Besides the values of $l_\odot$, $b_\odot$, $V_\odot$, and their standard errors we also give the number of galaxies used and the typical depth of each sample.

The trend of the solar apex on the sky shows an initial "stage of jumps" caused by small number statistics, and then

TABLE 1. The sample of galaxies and the solar apex solution.

k	Name	l	b	V_h	R	$l_\odot$	$b_\odot$	$V_\odot$	H	σ_V	V_{pec}
		galaxies				solar apex					
1	LMC	280.5	−32.9	324	0.05	—	—	—	—	—	46
2	SMC	302.8	−44.3	175	0.06	—	—	—	—	—	−30
3	DRACO	86.4	34.7	−296	0.08	—	—	—	—	—	−21
4	SCULPT	287.8	−83.2	148	0.08	60.3	18.1	366	—	—	107
5	SEX-sph	243.5	42.3	230	0.09	57.2	14.5	400	—	57	13
6	URSA MIN	105.0	44.8	−209	0.09	54.9	14.0	399	—	49	23
7	CARINA	260.1	−22.2	240	0.11	68.0	13.1	326	—	68	−65
8	FORNAX	237.3	−65.7	53	0.16	95.5	2.3	319	—	75	−64
9	LEO-2	220.1	67.2	70	0.22	95.0	1.8	320	—	68	−9
10	LEO-1	226.0	49.1	285	0.27	81.6	−0.2	341	—	80	133
11	PHOENIX	272.2	−69.0	56	0.42	85.2	−2.5	341	—	77	−67
12	N 6822	25.3	−18.4	−56	0.52	99.0	−4.8	353	—	77	74
13	SAGITT	21.1	−16.3	−78	0.57	99.1	−4.8	353	—	72	31
14	LGS-3 *)	126.8	−40.9	−281	0.58	100.4	−5.5	361	—	69	−78
15	N 185	120.8	−14.5	−251	0.62	97.4	+ 4.3	341	—	69	29
16	IC 1613	129.7	−60.6	−231	0.66	99.1	−5.8	350	—	68	−106
17	N 147	119.8	−14.3	−163	0.76	95.1	−4.6	325	—	77	120
18	N 221	121.2	−22.0	−203	0.76	93.3	−3.9	315	—	76	64
19	M 31	121.2	−21.6	−300	0.77	94.0	−4.2	319	—	74	−33
20	M 33	133.6	−31.3	−180	0.84	93.0	−3.7	316	—	72	28
21	N 205	120.7	−21.1	−233	0.85	92.5	−3.5	313	—	71	37
22	WLM	75.7	−73.6	−120	0.95	92.4	−3.8	314	—	69	−32
23	DDO 210 *)	34.1	−31.4	−137	1.00	92.9	−3.7	313	—	67	17
24	IC 10	119.0	−3.3	−344	1.04	93.6	−3.7	318	—	67	−50
25	N 55	332.9	−75.7	125	1.34	94.1	−1.9	320	—	69	83
26	SEX A	246.1	39.9	323	1.41	92.6	−2.6	327	—	70	92
27	SEX B	233.2	43.8	301	1.44	90.8	−3.3	333	—	72	112
28	LEO A	196.9	52.4	20	1.47	91.7	−2.9	332	—	71	−34
29	IC 5152	343.9	−50.2	121	1.50	92.7	−2.3	333	—	71	56
30	N 3109	262.1	23.1	403	1.54	92.7	−2.3	333	63	69	−8
31	P 621	351.5	−78.1	206	1.55	93.1	−1.6	330	98	69	82
32	P 71431 *)	11.9	−70.8	61	1.55	92.7	−1.8	332	84	69	−31
33	PEGASUS	94.8	−43.6	−183	1.75	92.8	−1.7	337	70	69	−67
34	N 1569	143.7	11.2	−89	1.84	92.9	−1.6	337	68	68	−20
35	UGCA 86	139.8	10.6	67	1.86	91.5	−2.4	332	85	71	152
36	IC 342	138.2	10.6	33	2.09	91.1	−2.7	331	92	71	109
37	MAFFEI-1	135.8	−0.6	15	2.10	90.8	−2.8	329	96	71	103
38	N 300 *)	299.2	−79.4	141	2.15	90.3	−3.6	326	88	71	−68
39	N 247	113.9	−83.5	159	m2.20	90.4	−3.5	326	90	70	35
40	N 253	97.4	−88.0	250	2.20	90.6	−3.0	327	94	71	103
41	UGCA 92	144.7	10.5	−99	2.21	91.4	−2.4	329	88	72	−60
42	GR-8 *)	310.8	77.0	213	2.24	90.4	−1.6	329	84	72	0
43	MAFFEI-2 *)	136.5	−0.3	−2	2.26	90.2	−1.6	328	86	71	72
44	BK3N	142.3	40.8	−40	2.79	90.0	−0.5	330	79	73	−77
45	K 52	143.8	33.0	113	2.95	90.0	−0.8	330	81	72	75
46	7 Zw 403 *)	127.8	37.3	−93	3.03	89.2	0.2	333	76	74	−93
47	DDO 53 *)	149.3	35.0	19	3.08	89.3	0.5	333	73	74	−53
48	N 2403	150.6	29.2	130	3.18	89.2	0.4	333	74	73	54
49	N 4236	127.4	47.4	0	3.24	88.7	0.8	334	72	73	−45
50	U 6572	157.6	66.4	230	p3.25	89.0	0.5	335	74	72	56
51	U 8320 *)	110.8	70.7	194	3.30	89.7	0.1	334	76	72	68
52	UGCA 105	148.5	13.7	111	3.31	89.5	0.1	334	76	71	52
53	Ho-9	142.0	41.1	46	3.41	89.5	0.3	334	75	71	−35
54	N 2366	146.4	28.5	99	3.45	89.5	0.3	334	75	70	23
55	N 3077	141.9	41.7	13	3.49	89.3	0.6	335	73	71	−74
56	M 82	141.4	40.6	202	m3.58	89.5	0.3	334	75	71	112
57	Ho-2	144.3	32.7	157	3.60	89.4	0.3	334	76	71	72
58	N 4945	305.3	13.3	560	m3.60	89.8	0.2	336	77	70	38
59	N 5102	309.7	25.8	467	m3.60	89.2	0.3	334	75	70	−21
60	N 5128	309.5	19.4	561	3.60	89.8	0.3	336	77	69	61
61	N 5206	310.2	14.1	577	m3.60	90.4	0.2	337	78	69	72
62	N 5237	311.9	19.2	373	m3.60	89.0	0.4	334	75	71	−119
63	N 5408	317.2	19.5	508	m3.60	89.3	0.4	335	76	70	36
64	P 47171	310.2	20.9	514	m3.60	89.3	0.4	335	76	70	19
65	P 48738	313.5	19.9	540	m3.60	89.6	0.3	335	76	69	55
66	M 81	142.1	40.9	−35	3.63	90.0	0.6	337	75	71	−131
67	U 4483	145.0	34.4	156	3.63	89.8	0.6	337	75	71	63
68	U 3755	206.0	9.7	317	p3.65	91.4	0.1	330	74	72	−80
69	U 8508 *)	111.1	61.3	62	3.68	91.0	0.4	332	74	71	−45
70	IC 2574	140.2	43.6	46	3.78	91.1	0.5	333	73	71	−61
71	N 1560	138.4	16.0	−36	3.84	91.4	0.3	334	72	72	−89
72	N 5253 *)	314.9	30.1	403	3.90	90.7	0.5	333	71	72	−80
73	K 73	136.9	44.2	115	4.04	90.7	0.5	333	71	71	−2
74	U 6541	151.9	63.3	246	p4.08	90.7	0.4	333	71	71	33
75	N 5264	315.7	31.7	477	m4.20	90.5	0.4	333	71	71	−20
76	P 48029	314.6	32.6	570	m4.20	91.0	0.3	333	72	71	71
77	P 48111	315.1	33.7	587	m4.20	91.5	0.2	334	73	71	92
78	P 48368	315.7	32.8	579	m4.20	92.0	0.1	334	73	71	84
79	DDO 187	25.6	70.5	154	4.40	90.9	0.7	338	73	72	−108
80	DDO 82 *)	137.9	42.2	40	4.48	91.1	0.7	340	72	72	−106
81	N 5236 *)	314.6	32.0	515	4.50	91.0	0.8	340	72	72	−7
82	U 9240 *)	82.0	64.5	152	4.53	90.8	0.8	341	71	71	−24
83	N 2976	143.9	40.9	3	4.57	91.3	0.9	341	70	73	−166
84	U 2905	174.3	−27.3	292	p4.66	91.3	0.8	341	70	73	−4
85	DDO 165	120.8	49.4	36	4.88	91.1	1.0	344	70	73	−118
86	N 5204 *)	113.5	58.0	203	4.92	91.2	0.9	343	70	73	21
87	IC 4182	107.7	79.1	320	4.95	91.3	0.8	343	70	73	33
88	N 4736	123.3	76.0	309	m4.95	91.4	0.7	342	70	72	30
89	U 7866	132.1	78.5	358	m4.95	91.5	0.6	342	71	72	61
90	U 7949	128.4	80.6	333	m4.95	91.5	0.5	342	71	72	29
91	N 3738	144.6	59.3	228	p5.16	91.6	0.5	342	71	72	−33
92	N 4605 *)	125.3	55.5	143	5.18	91.5	0.6	343	70	71	−64
93	N 5238 *)	107.4	64.2	232	5.18	91.5	0.5	342	70	71	8
94	N 5585	101.0	56.5	305	5.70	91.9	0.5	340	71	71	86
95	U 3860	177.8	23.9	353	p5.86	92.3	0.3	339	71	71	−43
96	U 8837	103.7	60.8	144	m6.58	91.7	0.4	342	70	72	−160
97	Ho-1	140.7	38.7	136	6.66	92.0	0.1	343	68	74	−164
98	M 101 *)	102.0	59.8	241	6.88	91.7	0.1	344	68	73	−78
99	N 5474 *)	100.8	60.2	277	7.18	91.6	0.1	345	68	73	−64
100	U 9405 *)	98.7	54.7	222	7.62	91.2	0.1	347	67	73	−123
101	U 288	118.6	−19.3	187	p7.69	91.2	−0.2	347	67	73	−78
102	N 5477 *)	101.6	59.5	304	7.73	91.1	−0.2	348	66	73	−73
103	N 3274	203.8	59.2	537	p8.00	91.4	−0.3	346	66	73	−92

Notes to Table 1. References for new distance estimates:

LGS-3	(TS,94)	DDO 210	(BCP,93)
P 71431	(BCP,93)	N 300	(FMHHMNS,92)
GR-8	(TSHD,95)	MAFFEI-2	(TK,94)
7 Zw 403	(KTS,94)	DDO 53	(KTS,94)
U 8320	(BCP,93)	U 8508	(KKT,94)
N 5253	(SSTLSPM,94)	DDO 82	(KTS,94)
N 5236	(SKEPSHMA,94)	U 9240	(KKK,94)
N 5204	(KKK,94)	N 4605	(KKK,94)
N 5238	(KKK,94)	M 101	(KKK,94)
N 5474	(KKK,94)	U 9405	(KKK,94)
N 5477	(KKK,94)		

a concentration of apex positions into the region $\{l_\odot=93°, b_\odot=-4°\}$ when the sample is approaching the LG boundary, followed by a transition to another predominant direction $\{91°, 0°\}$ when the whole Local Volume is considered. The behavior of the absolute value of the solar velocity towards the apex is drawn on the top of Fig. 2 as circles. Outside the LG the value of $V_\odot$ rises smoothly from 315 up to 345 km s^{-1}, showing small fluctuations when one or another galaxy group gets into the analysis. As one can see in Fig. 1 and Table 2, the old solar apex positions are spread over a region of $\sim 15°$ and lie systematically beside the concentration of new apex positions. Such difference is caused partially by the new data on radial velocities of dwarf galaxies: Leo 1 (Zaritsky *et al.* 1989), Phoenix (Carignan *et al.* 1991), Carina, and LGS-3, as well by a new approach to the data analysis.

To study the apex behaviour for the Galaxy center we corrected the radial velocities V_h for the Galaxy rotation, using the relation

$$V_g = V_h + V_a(\cos b \cos b_a \cos(l-l_a) + \sin b \sin b_a) \quad (3)$$

with the parameters of the solar apex from the first line of Table 2. Changing V_h into V_g in Eq. (2), we obtain a sequence of positions for the galactic apex relative to volumes of varying depth R_k. The Galaxy apex trajectory is shown in Fig. 3 as circles with indication of distances for some of them in Mpc. The location of M31 and other massive galaxies are marked by diamonds. As it follows from these data, for increasing R the Galaxy apex shifts toward M31, approaching it up to the minimum angular distance of 4°. Then, for $R>0.6$ Mpc, the apex shifts away from M31 to reach the asymptotic position $\{l=100°, b=-4°\}$ with an intermediate stop in the region $\{l=107°, b=-18°\}$. The velocity amplitude for the Galaxy center motion toward the running apex changes from the minimum value of (90 ± 2) km s^{-1} at $R=0.8-1.0$ Mpc up to (115 ± 5) km s^{-1} in the range of 4.5–8.0 Mpc (see squares on Fig. 2). Such a variation of the Galaxy apex parameters well fits the idea, that the nearby

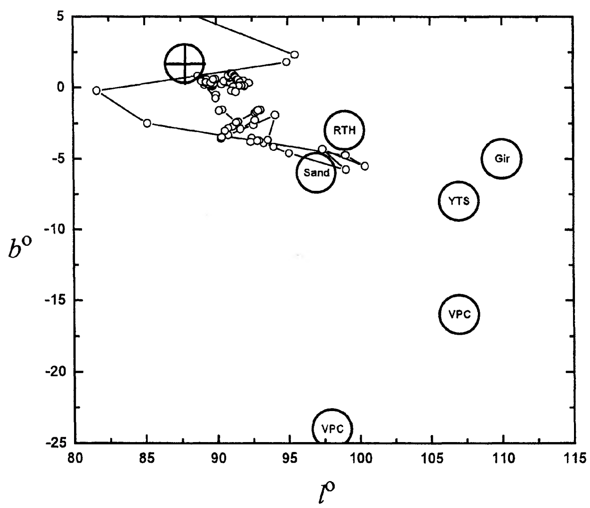

FIG. 1. Solar apex positions in galactic coordinates. The sequence of small circles connected with lines shows the apex shifts regarding to galaxy samples of different depth. Large circles are apex positions according to published data (see Table 2).

M31 group affects strongly the Galaxy motion (Yahil *et al.* 1977; Sandage 1986). Note that the peculiar velocity of the Galaxy toward M31 is about 3/4 of the radial velocity difference for these galaxies, whichis -122 km s^{-1}.

The trends of the apex with the distance, shown on Figs. 1–3, do not allow to establish if there is or not a continuous transition from the local apex to the global one determined by the dipole anisotropy of CMB. To check it we reduced the measured radial velocities of galaxies for the solar motion with respect to the LG centroid, using Eq. (3) with the apex parameters:

$$\{l_\odot=93°,\ b_\odot=-4°,\ V_\odot=316\ \text{km s}^{-1}\}. \quad (4)$$

The calculated apex position for the LG centroid are shown in Fig. 4 as small circles. The figures below some of circles give the depth of the sample, R_k, in Mpc. The nearby massive galaxies: Maffei 1+2, IC 342, M81, and M101 are shown on Fig. 4 as triangles, and two diamonds show the positions of the nearest cloud of galaxies in Canes Venatici and the center of the Local Supercluster in Virgo. As it can be seen, the Local Group apex sequence follows a rather intricate trajectory, lying far away from all known local mass concentrations. The absolute value of the LG velocity relative to volumes of different radius R is shown in Fig. 2 by the triangles. Over the whole range of distances the Local Group velocity turns out to be rather small and increase smoothly from 0 up to 40 km s^{-1}.

As it was mentioned above, de Vaucouleurs & Peters (1981, 1984) studied the behavior of the solar apex relative to different samples of galaxies with distance estimates from the luminosity index and the TF relation. Their parameters for the solar apexes, the number of galaxies used, and the average depth of each sample are listed at the bottom of Table 2. From these data, we derived the LG apex positions with respect to such deeper samples, and plotted them in Fig. 4 as large open circles.

TABLE 2. The solar apexes respect to nearby galaxies.

l (°)	b (°)	V (km/s)	n	R_{eff} Mpc	Reference
87.8	1.7	232	Gal.rotat.		(V,83)
107 ± 5	-8 ± 4	300 ± 22	11	1.5	(YTS,77)
97	-6	295	20	1.5	(S,86)
99 ± 4	-3 ± 3	311 ± 16	25	1.5	(RTH,87)
110 ± 6	-5 ± 6	280 ± 10	27	2.0	(G,86)
98 ± 6	-24 ± 7	342 ± 37	12	1.5	(VPC,77)
107 ± 6	-16 ± 4	336 ± 17	21	2.0	(VPC,77)
123 ± 19	23 ± 10	345 ± 70	93	9.6	(VP,81),A
125 ± 11	6 ± 5	338 ± 40	130	6.4	(VP,84),A
120 ± 14	27 ± 7	384 ± 60	137	12.2	(VP,84),B
138 ± 20	63 ± 10	267 ± 60	139	15.4	(VP,84),C
166 ± 26	23 ± 15	328 ± 130	133	19.2	(VP,84),D
155 ± 28	53 ± 17	352 ± 140	127	24.2	(VP,84),E
309 ± 31	45 ± 18	485 ± 220	112	36.0	(VP,84),F
264 ± 1	48 ± 1	370 ± 5	CMB		(KLS,93)

The numbers close to the circles give the LG velocity with respect to the apex in km s^{-1}. The last line in Table 2 gives the Sun velocity direction and value with respect to CMB frame of rest. Using a new apex (4), we find that the Local Group centroid moves in the CMB frame towards the point l=269°, b=+29° with a velocity of 635 km s^{-1} (the square on Fig. 4). As de Vaucouleurs & Peters (1984) already noted, for increasing values of R, the LG apex tends to shift toward the CMB point, and its velocity tends also to increase. The same conclusion was reached by Martin-Mirones & Goicoechea (1992) from a sample of 300 elliptical galax-

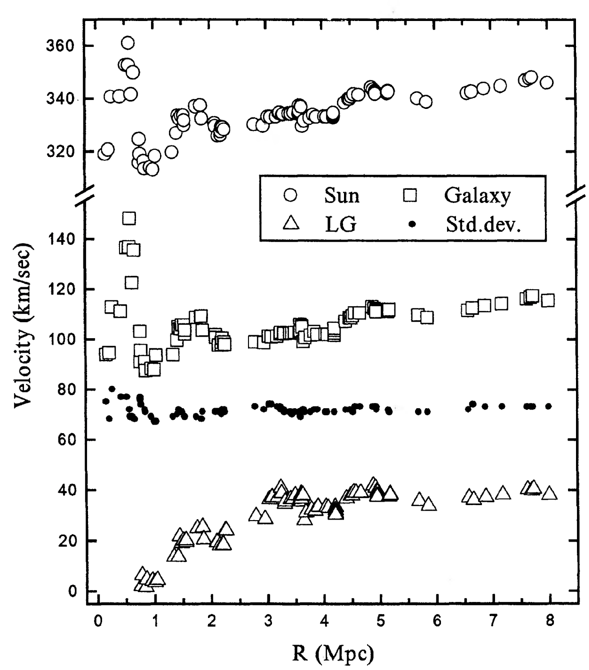

FIG. 2. Amplitudes of motion towards an apex for the Sun, the Galaxy, and the Local Group centroid as a function of the galaxy sample depth under consideration. Filled circles indicate a peculiar velocity dispersion for galaxies within different distance R.

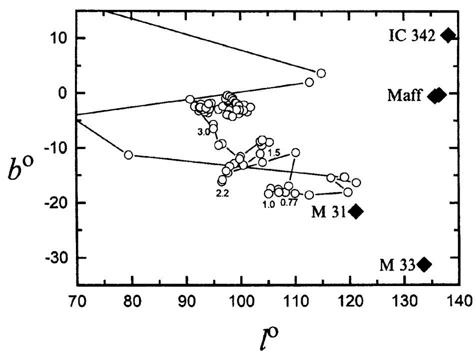

FIG. 3. The Galaxy apex trend with respect to volumes of different depth. Some quantities of R are marked by number beside the circles. The nearest massive galaxies are indicated by diamonds.

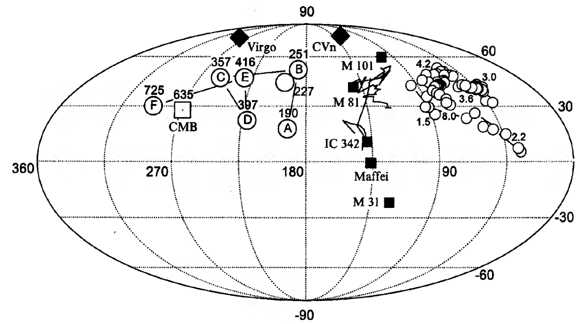

FIG. 4. The Local Group apex trends relative to nearby and moderately distant galaxies. Small circles are apex positions regarding to the samples of 1.5–8.0 Mpc by our data. Large circles indicate apexes for more distant samples considered by de Vaucouleurs & Peters (1984). Numbers beside them mean velocities toward apex in km s^{-1}. The square is the LG apex with respect to CMB. Triangles and diamonds are nearby galaxy system. Thin line indicates the LG apex drift under parameters $\{l_\odot=88°, b_\odot=-4°, V_\odot=316$ km s$^{-1}\}$.

ies having distances in a range of 10–55 Mpc. However, for the nearest subsample by de Vaucouleurs & Peters, which has $R_{\rm eff}=6.4$ Mpc, the LG apex stands rather far away from the apex derived for our complete sample. The comparison of these two almost independent sets of data shows a discrepancy which needs to be clarified by new photometric distances of galaxies having $R>5$ Mpc.

It should be noted, however, that the amplitude of the LG motion toward the running apex is rather low thus explaining why even a small random variation in the apex parameters can lead to a significant displacement of the apex on the sky. For instance, by changing the apex longitude in Eq. (4) on 5°($l=93°\rightarrow 88°$), we can derive a new running apex which is traced in Fig. 4 as a thin line. When R increases, this new apex drifts along the Local Supergalactic equator passing nearby the M81 group. It is obvious, that our present knowledge of the behavior of the LG apex relative to galaxies with distances of 5–10 Mpc remains still very imprecise due to the paucity of reliable observational data.

4. THE VERY NEARBY VELOCITY FIELD

In solving the system of Eq. (2), we defined a running apex parameters, as well a running value of the Hubble constant, H_k with respect to the centroid of k nearest galaxies. The resulting values are given in the column H of Table 1 and in Fig. 5. The $H(R)$ dependence presents a sharp maximum of ~90 km s^{-1} Mpc^{-1} at a distance of ~2 Mpc, then decreases to a value of (70–65) km s^{-1} Mpc^{-1} at the edges of the volume considered. Such a behavior of the local Hubble parameter is rather unexpected and was previously unknown. For instance, de Vaucouleurs & Peters (1981, 1984) found H to be constant in the range 6–36 Mpc. Bottinelli *et al.* (1986) found instead $H(R)$ to be increasing on a scale of ~20 Mpc but explained it as an observational selection effect (Malmquist bias). Tully (1988a) and Giraud (1990) found an increase of H from ~63 up to 90 km s^{-1} Mpc^{-1} over the distance range of 7–30 Mpc and ascribed it to a real phenomenon, caused by a deceleration of the Hubble expansion due to the massive Local Cloud. Moreover, the mass of the Local Group has to lead to an increase of $H(R)$, appreciable inside a distance of $R=1$–2 Mpc (Sandage 1986). Therefore, the observed decrease of $H(R)$ on Fig. 5 seems like a puzzle.

However, as it follows from the data of Table 1 the main contribution to the peak in $H(R)$ comes from galaxies in the two groups: IC 342+Maffei (four galaxies) and Sculptor (three ones). A case of systematic errors in their distance may be considered as probable reason of the $H(R)$ peak. A possible explanation of the shortened time scale H^{-1}, inside the volume of $R<3$ Mpc could be found also in the "Local Big Bang" scenario, proposed by Zheng *et al.* (1991) and Valtonen *et al.* (1993). it is worth noticing that $H(R)$ peak in Fig. 5 becomes a little shallower if the galactocentric distance be replaced onto the distance measured from the mass center of Milky Way and M31.

At the last we should remember that our sample have been restricted with the condition of $V_0<500$ km s^{-1}. In a velocity-limited sample of galaxies ordered by measured distances their measurement errors will create a systematic bias which can be responsible for the downward trend of H on $R>5$ Mpc.

Besides the deviation from the ideal homogeneous Hubble expansion seen in the radial direction, the local velocity field shows also signs of angular anisotropy. Assuming for the Local Volume galaxies the median solar apex

$$\{l_\odot=91°,\ b_\odot=0°,\ V_\odot=334 \text{ km s}^{-1}\}, \tag{5}$$

and taking into account the trend of $H(R)$, we calculated for each galaxy its peculiar radial velocity $V_{\rm pec}$, with respect to a comoving frame of rest, and also the corresponding dispersion of peculiar velocities σ_v^2, within a sphere of radius R. These quantities are represented in the last two columns of Table 1. The distribution of peculiar velocities for the 103 galaxies is shown on Fig. 6 in Cartesian Supergalactic coordinates. As suspected by Karachentsev (1994), the galaxies located far away from the LSC plane have preferably negative peculiar velocities. New distance measurements for galaxies with |SGZ|>1 Mpc confirm this effect: among 20 such galaxies there are only 4 with $V_{\rm pec}>0$, and 3 of them are members of the M101 group.

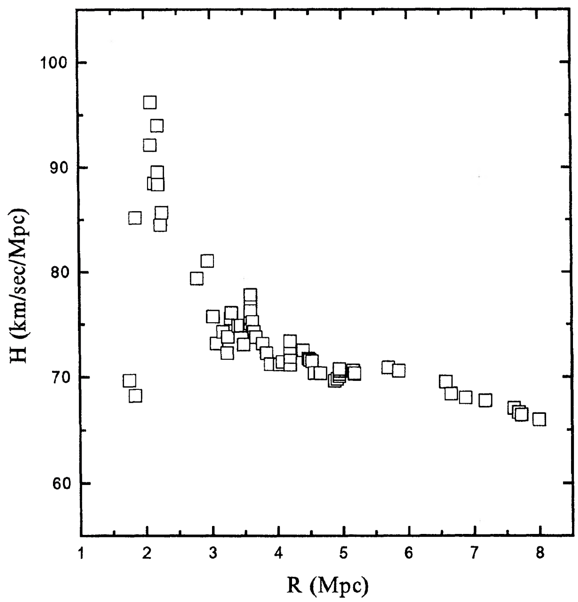

FIG. 5. A running local value of Hubble parameter regarding to galaxy samples of different depth.

On the average the deceleration effect along the SGZ axis may be expressed by the regression

$$\langle V_{\rm pec} \rangle = -(18 \pm 5)|{\rm SGZ}| \tag{6}$$

in km s^{-1}.

The distribution of peculiar velocities in the Supergalactic plane shows also signs of anisotropy: in the direction of the LSC center (axis "+SGY") an excess of negative peculiar velocities. On a scale of about 30 Mpc this feature had already been noticed by de Vaucouleurs & Bollinger (1979), and by de Vaucouleurs & Peters (1985). Using a sample of 500 galaxies the latter authors drew a map of the Hubble parameter distribution along the LSC plane, finding a region of low values, namely, $H \simeq 70$ km s^{-1} Mpc^{-1} (lower than the mean of 100 km s^{-1} Mpc^{-1}) in the direction of SGL$\simeq 90°$ (toward Virgo). The direction and the amplitude of this effect agrees well with our data, if the different scales are taken into account.

The angular anisotropy is usually named "Local Velocity Anomaly" (LVA) and has been matter of debate among different authors. Giraud (1990) explained the VLA phenomena as a gravitational deceleration of galaxies inside the Local Cloud. Han & Mould (1990) interpreted the LVA as due to a repulsion of the local volume galaxies induced by the Local Void, which occupies the region $\{l<90°, |b|<60°\}$. Tully *et al.* (1992) relate the LVA to the existence of discrete clouds: Coma + Sculptor and Leo Spur that are approaching each other with a velocity of $\sim$200 km s^{-1}.

We wish to stress here that the dispersions of peculiar velocities are surprisingly constant irrespective the radius of the sphere taken into account in order to compute σ_v. As one can see from the column σ_V of Table I and Fig. 2, relative variations of σ_v do not exceed 3% outside the Local Group. Even the crossing of the "zero velocity surface" at $R_0=1.5$ Mpc does not lead to a discontinuity in the $\sigma_v(R)$ dependence. Moreover, the dispersion of peculiar velocities is almost the same for giant ($M>3\times10^{11}\ \mathcal{M}_\odot$) galaxies and for dwarf ($M<3\times10^{7}\ \mathcal{M}_\odot$) ones. A temperature of a "gas" of galaxies defined by the value of $\sigma_v=(72\pm2)$ km s^{-1} seems to be an important quantity probably related with the initial conditions of formation for the small-scale structures observed in the Local Universe.

5. 3D VIEWING OF THE LOCAL VOLUME

Over the last four years the number of galaxies with individual photometric distance moduli has increased by about a factor of 3. Nevertheless, the relative number of such galaxies does not even reach 50% in the Local Volume and very few galaxies have been measured in the southern hemisphere. This introduces an anisotropic selection when one attempts to get a 3D map of the Local Volume. Using the radial velocities of galaxies, corrected for the solar motion toward the median apex (5), and by taking into account a correction for the anisotropy (6), we determined their kinematic (Hubble) distances, assuming for the Hubble "constant" the average local value $H=71$ km s^{-1} Mpc^{-1}. The results are presented on Fig. 7 in the Cartesian Supergalactic coordinates. The upper panel of Fig. 7 shows a projection of the LV galaxies onto the Supercluster plane. The lower panel gives an edge-on view. The circle radius corresponds to 8 Mpc. The galaxies from Table 1 with measured photometric distances are drawn as filled squares, and objects with kinematic distances are marked by crosses. We see on the map some regions (Canes Venatici Cloud, Leo Spur) which are almost empty of galaxies with individual distance moduli. This is rather surprising and calls for a better coverage of photometric distances for the Local Volume.

For a comparison, in Fig. 8 we reproduce the distribution of galaxies obtained by Tully (1988b) within the same volume. Distances were estimated by Tully via their radial velocities after correction for the solar motion {300 km s^{-1}; $l=90°$, $b=0°$}, and for a component of the Virgocentric flow (Tully & Shaya 1984; $H=75$ km s^{-1} Mpc^{-1}). In the overall view Figs. 7 and 8 present a similar distribution of galaxies. However, one can recognize some significant differences in their pattern. The distribution of galaxies from Tully's catalog appears like more smoothed in both projections. The LV map drawn up with individual photometric distances finds instead a sharper concentrations of galaxies into groups, as well as towards the LSC plane. Some voids are more clearly visible in Fig. 7, and in particular the empty volume between the LG and M81 group (Karachentsev *et al.* 1994b), and the gap between the Canes Venatici cloud and Leo Spur (Tully 1988b).

It needs to be stressed, however, that the large number of galaxies in the LV lacking accurate distance determinations based on photometric methods may affect our present understanding of its small scale structure. Furthermore, a reliable knowledge of 3D pattern of the LV is needed in order toprovide a reliable observational ground for N-body simulations of the local velocity field and for studies of Dark Matter.

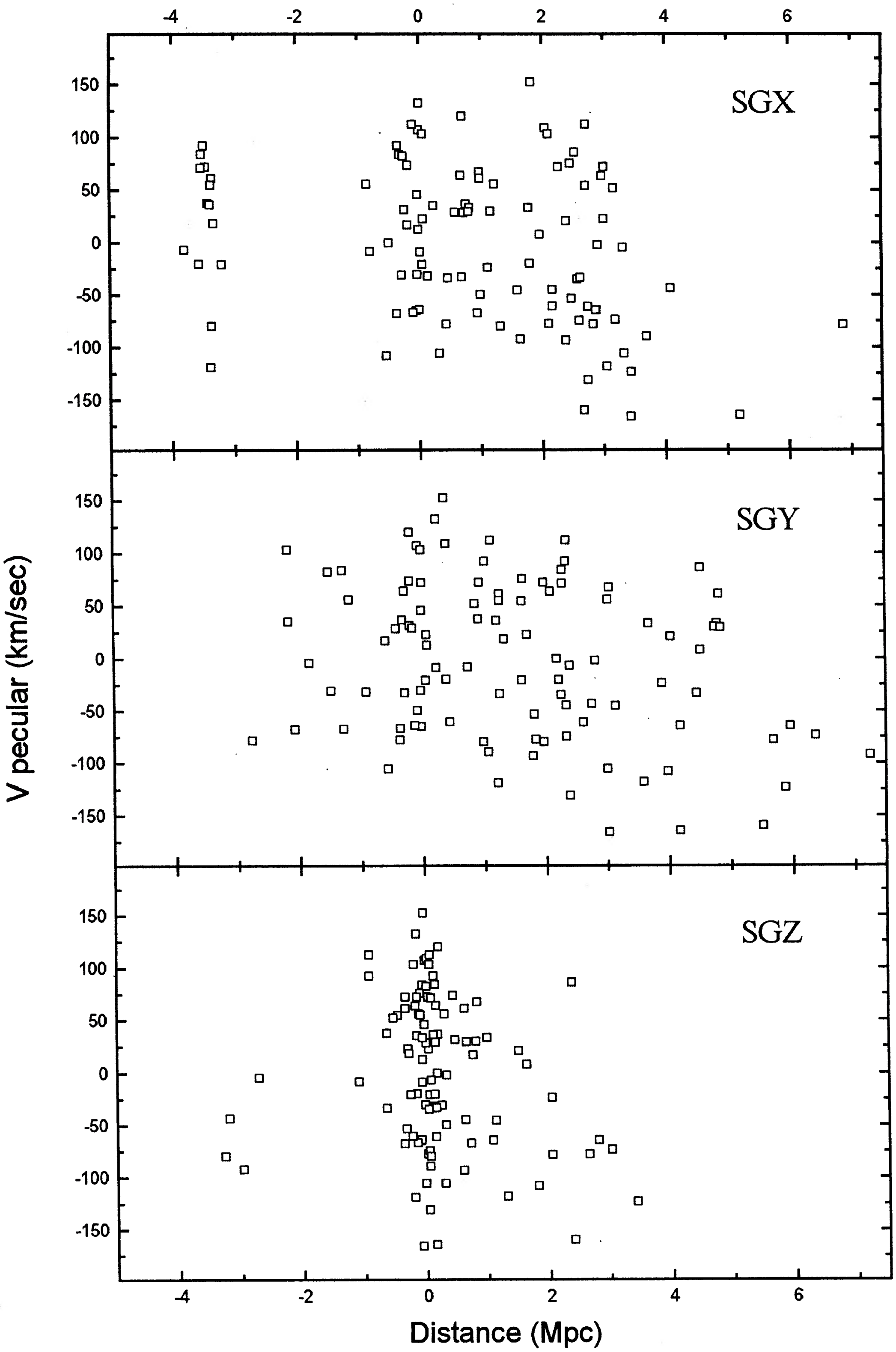

FIG. 6. A local field of peculiar radial velocities in the Cartesian Supergalactic coordinates.

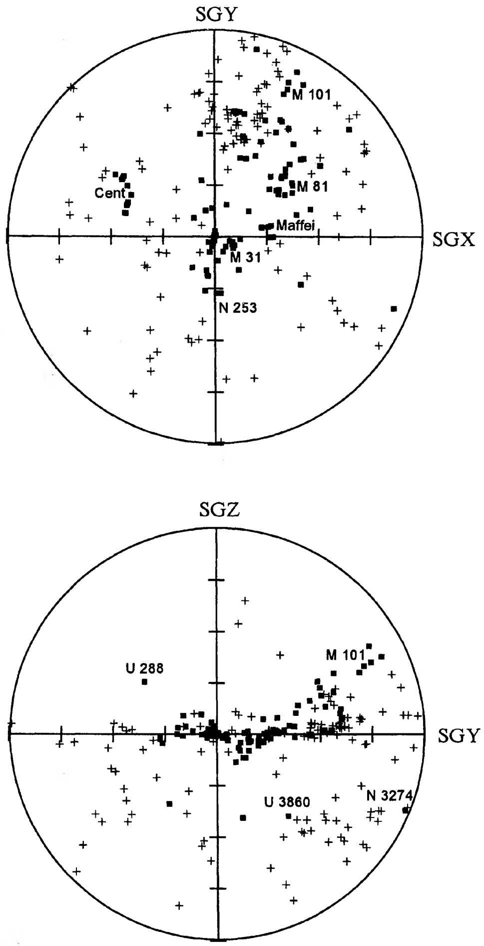

FIG. 7. Distribution of 221 galaxies in the Local Volume with photometric (squares) and kinematic (crosses) distances.

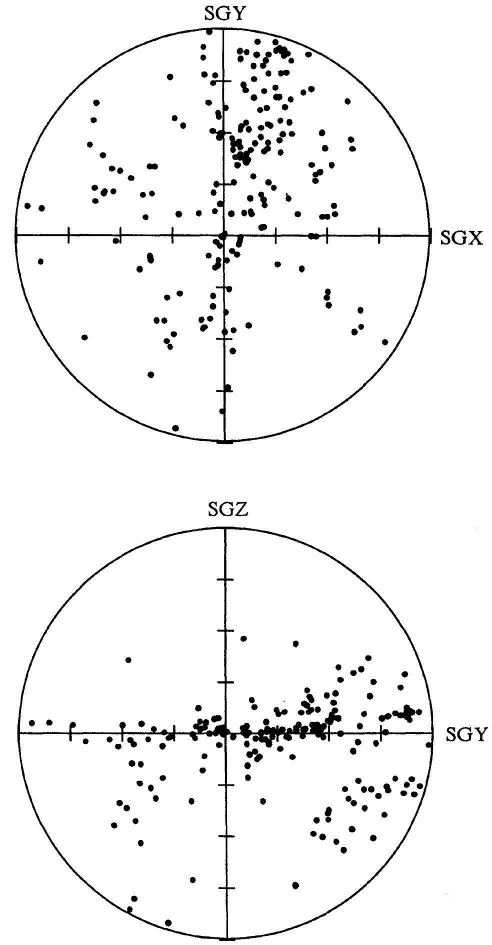

FIG. 8. Distribution of 209 galaxies from Tully's catalog in the same volume of $R=8$ Mpc.

6. CONCLUSIONS

The new observational data on distances and radial velocities for nearby galaxies has called for a revision of the solutions for the Sun motion with respect to different frames of rest. Using a more or less homogeneous and representative sample of galaxies having photometric distance moduli we estimated the parameters of the running solar apex as a function of volumes with increasing radii. The data analysis allows us to formulate such conclusions.

• An optimum direction and velocity of the Sun motion relative to the Local System galaxies may be expressed by the parameters $\{l_{\odot}=93°, b_{\odot}=-4°, V_{\odot}=316$ km s$^{-1}\}$ with formal standard errors of 2° and 5 km s^{-1}. Using these parameters, which are quite different from previous ones (see Table 2), the center of our Galaxy moves with the velocity of 90 km s^{-1} toward the point $l=107°$, $b=-18°$, which is 14° away the M31.

• When the depth of the considered volume increases from 1.0–1.5 Mpc up to 4–8 Mpc, the solar apex shifts a little towards: $\{l_{\odot}=91°, b_{\odot}=0°, V_{\odot}=334$ km s$^{-1}\}$. Whereas the apex of the LG centroid reveals a complicate wandering in the region $\{l=40°-100°, b=0°-+60°\}$. The LG centroid velocity does not exceed 40 km s^{-1} with respect to samples of the LV galaxies having different depth R. The small amplitude of the LG apex motion might explain its chaotic wandering on the sky. de Vaucouleurs & Peters (1984) considered the behavior of the LG apex with respect to more distant galaxies with $R=6$–36 Mpc. According to their data, the LG apex, at increasing R, drifts towards the CMB apex. However, both parts of the apex trace look quite separate on the common distance interval for them, namely ~6 Mpc. To understand the reason of such disagreement we need new data on more distant galaxies distributed more uniformously over the sky.

• Just outside the "zero velocity surface" of the Local System, namely, at $R\sim2$ Mpc, the Hubble parameter reaches the maximum value, (90 ± 5) km s^{-1} Mpc^{-1}, and then decreases smoothly down to (70–65) km s^{-1} Mpc^{-1}. Such a behavior of $H(R)$ seems abnormal, unless it is due to either an observational selection or to errors in the distance moduli of those galaxies which are in the immediate neighborhood of the LG.

• When the Hubble component is removed the residual radial velocities of galaxies present evident signs of anisotropy. In the Local Supercluster plane there is a prevalence of negative peculiar velocities in the direction of +SGY, i.e., $L \simeq 90°$. This feature of the very nearby velocity field behaves like the well-known phenomena "Local Velocity Anomaly" found on the scale of 10–30 Mpc. Among the different proposed explanations of this effect, we believe that the gravitational retarding of cosmic expansion within the Local Cloud (Tully 1988a; Giraud 1990) is more likely.

• Besides the "Local Anomaly" feature, seen in the LSC plane, peculiar velocities of the galaxies reveal also anisotropy in a transverse direction. Cosmologic expansion of the Local "pancake" along the Z direction takes place with a rate which is 30% slower as in the plane. This circumstance becomes clear just at present, when individual photometric distances are measured for two dozen of galaxies situated on high supergalactic latitudes. Anisotropy of the local value of Hubble parameter, namely, $H_x:H_y:H_z:=70:(60^+/80^-):50$ km s^{-1} Mpc^{-1}, arises obviously from the local gravitational field.

• The peculiar velocity dispersion of the galaxies remains practically constant regardless the radius of the sample volume. Its value, $\sigma_v=(72\pm2)$ km s^{-1}, is approximately the same as for dwarf as well for giant galaxies. Together with virial velocities, both residual coherent velocities of field galaxies, and also distance measurement errors give a contribution into the σ_v. Therefore, a constancy of such combination of different quantities seems rather unexpected.

• By using more precise parameters of the solar apex and by taking into account the local anisotropy we can use the radial velocities of nearby galaxies as a much more reliable distance indicator. Combining such improved kinematic distances with known photometric moduli, we constructed the 3D map of the Local Volume. Its comparison with the former map from Tully's catalog reveals the "fine grain" in much better detail. The existence of some structural details, like the minivoid of 2 Mpc situated between the Local System and M81 group, may be considered as an efficient means to prove different scenarios of galaxy formation. One should remember however, that a real accuracy of kinematic distances consists of ~1 Mpc due to mentioned peculiar velocity dispersion. Therefore a systematic measurement of photometric distances for nearby galaxies remains still as an actual observing task both for northern and southern telescopes.

We consider the discussed properties of local coherent motions as only preliminary ones until a better completeness of the LV sample and its whole-sky coverage will be achieved.

Our paper benefited from useful discussions with M. Capaccioli, G. Longo, and G. Richter. We thank the referee, R. B. Tully, for his valuable comments. This work was supported by ESO C&EE Programme Grants No. A-02-16 and No. B-04-034.

REFERENCES

Aaronson, M., Huchra, J., Mould, J., Shechter, P. L., & Tully, R. B. 1982, ApJ, 258, 64
Bottinelli, L., Gouguenheim, L., Paturel, G., & Teerikorpi, P. 1986, A&A, 156, 157
Bresolin, F., Capaccioli, M., & Piotti, G. 1993, AJ, 105, 1779 (BCP93)
Capaccioli, M., & Piotto, G. 1995 (in press)
Carignan, C., Demers, S., & Cote S. 1991, ApJ, 381, L13
Cook, K. H., Aaronson, M., & Illingworth, G. 1986, ApJ, 301, L45
de Vaucouleurs, G. 1983, ApJ, 268, 451 (V83)
de Vaucouleurs, G., & Bollinger, G. 1979, ApJ, 233, 433
de Vaucouleurs, G., de Vaucouleurs, A., Buta, R. G., Corwin, H. G., Fouqué, P., & Paturel, G. 1991, Third Reference Catalog of Bright Galaxies (Springer, New York) (RC3)
de Vaucouleurs, G., & Peters, W. L. 1981, ApJ, 248, 395 (VP81)
de Vaucouleurs, G., & Peters, W. L. 1984, ApJ, 287, 1 (VP84)
de Vaucouleurs, G., & Peters, W. L. 1985, ApJ, 297, 27
de Vaucouleurs, G., Peters, W. L., & Corwin, H. G. 1977, ApJ, 211, 319 (VPC77)
Dressler, A., Faber, S. M., Burstein, D., Davies, R. L., Lynden-Bell, D., Terlevich, R. J., & Wegner, G. 1987, ApJ, 313, L37
Freedman, W. L., Madore, B. F., Hawley, S. L., Horowitz, I. K., Mould, J., Navarrete, M., & Sablmen, S. 1992, Caltech Astrophys. Abstracts 2, 9 (FMHHMNS92)
Giraud, E. 1986, A&A, 170, 1 (G86)
Giraud, E. 1990, A&A, 231, 1
Han, M., & Mould, J. 1990, ApJ, 360, 448
Hoffman, G. L., & Salpeter, E. E. 1982, ApJ, 263, 485
Huchtmeier, W. K. 1994 (private communication)
Karachentsev, I. D. 1994, A&A Trans, 6, 1
Georgiev, Ts. B., Karachentsev, I. D., & Tikhonov, N. A. 1996 (in press)
Karachentsev, I. D., Kopylov, A. I., & Kopylova, F. G. 1994a, Bull. Spec. Astrophys. Obs., 38, 15 (KKK94)
Karachentsev, I. D., & Tikhonov, N. A. 1994, A&A, 286, 718
Karachentsev, I. D., Tikhonov, N. A., & Sazonova, L. N. 1994b, A&AS, 106, 555
Kraan-Korteweg, R., & Tammann, G. 1979, Astron. Nach., 300, 181
Kogut, A., Lineweaver, C., Smoot, G. F., *et al.* 1993, ApJ, 419, 1 (KLS93)
Lauer, T. R., & Postman, M. 1992, BAAS, 24, 1264
Lynden-Bell, D., Faber, S. M., Burstein, D., Davies, R. S., Dressler, A., Terlevich, R. J., & Wegner, G. 1988, ApJ, 326, 19
Madore, B. F., & Freedman, W. L. 1991, PASP, 103, 933
Martin-Marones, J. M., & Goicoechea, L. J. 1992, A&A, 253, 3
Mathewson, D. S., Ford, V. L., & Buchorn, M. 1992, ApJS, 81, 413
Paturel, G., Bottinelli, L., Fouqué, P., & Gouguenheim, L. 1992, Catalogue of Principal Galaxies: PGC-ROM (Observatoire de Lyon)
Peebles, P. J. E. 1988, ApJ, 332, 17
Peebles, P. J. E. 1989, JRASC, 83, 363
Peebles, P. J. E. 1994, ApJ, 429, 43
Richter, O. G., Tammann, G. A., & Huchtmeier, W. K. 1987, A&A, 171, 33 (RTH87)
Sandage, A. 1986, ApJ, 307, 86 (S86)
Sandage, A., Saha, A., Tammann, G. A., Labhardt, L., Schwengeler, H., Panagia, N., & Maccetto, F. D. 1994, ApJ, 423, L13 (SSTLSPM94)
Schmidt, B. P., Kirshner, R. P., Eastman, R. G., Phillips, M. M., Suntzeff, N. B., Hamuy, M., Maza, J., & Aviles, R. 1994, ApJ, 432, 42 (SKEPSHMA94)
Tikhonov, N. A., & Karachentsev, I. D. 1994, Bull. Spets. Astrophys. Obs., 38, 3 (TK94)
Tikhonov, N. A., & Sazonova, L. N. 1994, A&A (in press) (TS94)
Tolstoy, E., Saha, A., Hoessel, J. G., & Danielson, G. E. 1995, AJ, 109, 579 (TSHD95)
Tonry, J. M., & Davies, M. 1981, ApJ, 246, 680
Tully, R. B. 1988a, Nature, 334, 209
Tully, R. B. 1988b, Nearby Galaxies Catalog (Cambridge University Press, Cambridge)

Tully, R. B., & Fisher, J. R. 1977, A&A, 54, 661
Tully, R. B., & Shaya, E. J. 1984, ApJ, 281, 31
Tully, R. B., Shaya, E. J., & Pierce, M. J. 1992, ApJS, 80, 479
Valtonen, M. J., Byrd, G. G., McCall, M. L., & Innanen, K. A., 1993, AJ, 105, 886
Yahil, A., Tammann, G. A., & Sandage, A. 1977, ApJ, 217, 903 (YTS77)
Zaritsky, D., Olszewski, E. W., Schommer, R. A., *et al.* 1989, ApJ, 345, 759
Zheng, J. A., Valtonen, M. J., & Byrd, G. G. 1991, A&A, 247, 20